Article

CK2 Phosphorylation Is Required for Regulation of Syntaxin 1A Activity in Ca^{2+}-Triggered Release in Neuroendocrine Cells

Noa Barak-Broner [1,†], Dafna Singer-Lahat [2,†], Dodo Chikvashvili [2] and Ilana Lotan [2,3,*]

[1] Department of Neurobiology Biochemistry & Biophysics, The George S. Wise Faculty of Life Sciences, Tel Aviv University, Ramat Aviv, Tel Aviv-Yafo 69978, Israel; noabara1@mail.tau.ac.il

[2] Department of Physiology and Pharmacology, Sackler School of Medicine, Tel Aviv University, Ramat Aviv, Tel Aviv-Yafo 69978, Israel; daflahat@tauex.tau.ac.il (D.S.-L.); dodoc@tauex.tau.ac.il (D.C.)

[3] Sagol School of Neuroscience, Tel Aviv University, Ramat Aviv, Tel Aviv-Yafo 69978, Israel

[*] Correspondence: ilotan@tauex.tau.ac.il

[†] Both authors contributed equally to this work.

Abstract: The polybasic juxtamembrane region (5RK) of the plasma membrane neuronal SNARE, syntaxin1A (Syx), was previously shown by us to act as a fusion clamp in PC12 cells, as charge neutralization of 5RK promotes spontaneous and inhibits Ca^{2+}-triggered release. Using a Syx-based FRET probe (CSYS), we demonstrated that 5RK is required for a depolarization-induced Ca^{+2}-dependent opening (close-to-open transition; CDO) of Syx, which involves the vesicular SNARE synaptobrevin2 and occurs concomitantly with Ca^{2+}-triggered release. Here, we investigated the mechanism underlying the CDO requirement for 5RK and identified phosphorylation of Syx at Ser-14 (S14) by casein kinase 2 (CK2) as a crucial molecular determinant. Thus, following biochemical verification that both endogenous Syx and CSYS are constitutively S14 phosphorylated in PC12 cells, dynamic FRET analysis of phospho-null and phospho-mimetic mutants of CSYS and the use of a CK2 inhibitor revealed that the S14 phosphorylation confers the CDO requirement for 5RK. In accord, amperometric analysis of catecholamine release revealed that the phospho-null mutant does not support Ca^{2+}-triggered release. These results identify a functionally important CK2 phosphorylation of Syx that is required for the 5RK-regulation of CDO and for concomitant Ca^{2+}-triggered release. Further, also spontaneous release, conferred by charge neutralization of 5RK, was abolished in the phospho-null mutant.

Keywords: syntaxin; CK2 phosphorylation; PC12 cells; exocytosis; amperometry; FRET; evoked release

1. Introduction

Ca^{2+}-triggered exocytosis is a fundamental cellular process mediated by the SNARE proteins, syntaxin 1A (Syx), synaptobrevin2 (Syb2), and SNAP-25 [1,2]. The plasma membrane (PM) SNARE, Syx, exists in two alternative conformations: a 'closed' conformation in which the SNARE motif is blocked by the Habc-domain [3], and an 'open' conformation in which the SNARE motif is exposed. In the 'open' conformation Syx can participate in the formation of SNARE complexes [4].

The very N terminal end of the Syx protein contains a highly conserved domain of 27 amino acids (N-peptide) [5], whose binding to the auxiliary SM protein Munc18-1 is essential for fusion [6–8]. In addition, the N-peptide, harbors a specific region of interest at Ser-14 (S14), which is the sole target in Syx for phosphorylation by casein kinase 2 (CK2) [9,10], a pleiotropic constitutively active serine/threonine protein kinase with particularly high levels in brain [11].

Many phosphoproteins participate in vesicle exocytosis. A number of observations over the past few years have suggested a potential role for CK2 phosphorylation of S14 in Syx in the direct modulation of exocytosis: (i) S14 phosphorylation increased through development in parallel with synapse development and maturation in rat brains [12];

(ii) S14 phosphorylation enhanced the interaction between Syx and synaptotagmin1 (Syt1) in vitro [13]; (iii) modification of S14 was found to play a role in a specific mode of the Syx-Munc18-1 interactions, affecting vesicle immobilization and exocytosis in PC12 cells [10].

Another structural determinant that is important for the activity of Syx in exocytosis is the polybasic stretch of five lysines and arginines (5RK) located at the juxtamembrane linker region that connects the SNARE motif and the transmembrane domain (TMD). This 5RK region was recognized as a lipid binding domain that plays a critical role in determining the energetics of SNARE-mediated fusion events [14] and is essential for lipid mixing and for the transition from hemifusion to full fusion in liposomes [15]. In PC12 cells, electrostatic interactions of 5RK with PI(4,5)P2 (PIP2) are thought to mediate the clustering and segregation of Syx into distinct microdomains where synaptic vesicles undergo exocytosis [16–18], possibly by serving as molecular beacons for vesicle docking by a Syt1 interaction with 5RK through PIP2 [19]. Similarly, electrostatic interactions between 5RK and PI(3,4,5)P3 have also been suggested to facilitate Syx clustering [20].

Previously, in an attempt to gain insights into the domain-specific-secretion-related functioning of Syx, we constructed a Syx-based fluorescence resonance energy transfer (FRET) probe, which allowed us to resolve a depolarization-induced Ca^{2+}-dependent conformational close-to-open transition (opening) of Syx that results from Ca^{2+} entry through voltage gated Ca^{2+} channels [21]. This Ca^{2+}-dependent opening (CDO) was accompanied by Ca^{2+}-triggered release, both in PC12 cells [21] and hippocampal neurons [22]. Notably, CDO was absolutely dependent on intact 5RK [21] and on plasma membrane PIP2 [23]. Further, our results suggested that the role of 5RK in exocytosis may be more central than has been previously demonstrated [14,17,20]. Indeed, amperometric analysis in PC12 cells revealed that charge neutralization of 5RK promoted spontaneous release and inhibited Ca^{2+}-triggered release, indicating that 5RK acts as a fusion clamp, making release dependent on stimulation by Ca^{2+} [23].

This current report identifies phosphorylated S14 as a significant molecular determinant in Syx that causes CDO to possibly occur within a vesicular setting in which it is absolutely dependent on the presence of intact 5RK, thereby supporting catecholamine release. We propose a model that describes the roles of phosphorylated S14 and 5RK and their interplay in exocytosis. This study is the first report to directly link in vivo CK2 phosphorylation and the activity of Syx as important for exocytosis.

2. Results

Previously, we used a Syx-based FRET probe, CSYS (Figure 1A), which reports Ca^{2+}-dependent close-to-open transition of Syx in response to high K+ (hK) depolarization (termed: Ca^{2+}-dependent opening; CDO), to reveal that the polybasic juxtamembrane 5RK stretch of Syx is essential for CDO and consequently for Ca^{2+}-triggered release [23]. Here, acknowledging the potential relevance of CK2-induced S14 phosphorylation of Syx to exocytosis (see Introduction), we used dynamic FRET and amperometry analyses to explore the possibility that S14 phosphorylation is involved in the molecular/cellular events that endow 5RK its central role.

2.1. S14 Phosphorylation of CSYS Is the Molecular Determinant That Makes 5RK Essential for CDO

First, using S14 phospho-specific antibody in a Western blot analysis, we established that in the PC12 cells used in our experiments endogenous Syx is S14 phosphorylated (Figure 1B(a)). Also, CSYS, exogenously expressed in the same cell, is S14 phosphorylated (Figure 1B(b)). The extent of phosphorylation of CSYS is similar to that of Syx, as determined in the heterologous expression system of *Xenopus* oocytes (Figure 1B(c)).
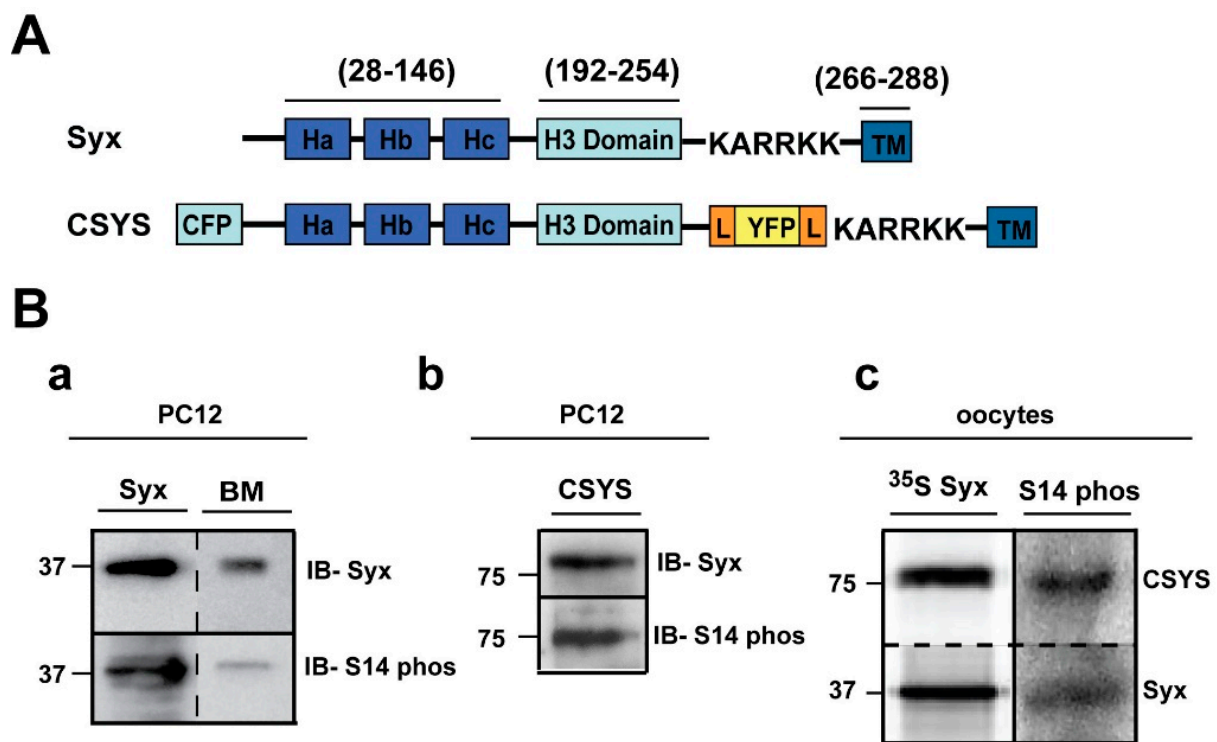
Figure 1. Syx and CSYS are targets for CK2 phosphorylation. (**A**) Domain structure of Syx and the CSYS FRET probe. (**B**) CSYS is a target for CK2 phosphorylation similarly to native Syx. (**a**) Native PC12 cells were immunoprecipitated with anti-Syx antibody and immunoblotted either with anti-Syx antibody (*IB-Syx*; upper panel) or with Syx S14 phospho-specific antibody (*IB- S14 phos*; lower panel). Brain membranes (BM) were loaded as a control. (**b**) Following immunoprecipitation with anti-YFP antibody, proteins of PC12 cells transfected with CSYS were subjected to Western blot analysis with either anti-Syx antibody (*IB-Syx*; upper panel) or with Syx S14 phospho-specific antibody (*IB-S14 phos*; lower panel). Molecular markers are shown on the left. (**c**) *Xenopus* oocytes expressing CSYS and Syx proteins were immunoprecipitated with anti-Syx antibody (^{35}*S Syx*; left panel) and immunoblotted with Syx S14 phospho-specific antibody (*IB-S14 phos*; right panel).

Next, we set to explore the possible involvement of S14 phosphorylation in CDO using the S14 phospho-null mutant CSYS;S14A (Figure 2A; S14 was mutated to alanine to prevent phosphorylation by CK2 [10]). We have previously defined CDO in CSYS expressing cells, using dynamic FRET analysis, as the reduction in the F_{YFP}/F_{CFP} ratio (FRET ratio), reporting a close-to open transition, that occurs in response to hK depolarization and is blocked by the voltage-gated Ca^{2+}-channel blocker, cadmium (Cd)[21]. Here, monitoring the FRET ratio reduction in response to hK depolarization in CSYS;S14A expressing cells, we found that it was similar to that monitored in parallel in CSYS expressing cells (Figure 2B(a)) and consisted of a fraction (CDO) that was blocked by 200 μM Cd (Figure 2B(b); F(79,6083) = 15.116, *p* < 0.0001, ANOVA with repeated measures). This analysis suggested that CSYS;S14A undergoes CDO, similarly to CSYS.

An absolute requirement of intact 5RK for CDO was previously demonstrated with the 5RK charge neutralization mutant, CSYS-5RK/A (the five basic residues replaced with alanines), in which the FRET ratio reduction in response to hK depolarization was smaller than that in CSYS and resistant to Cd block; namely the neutralization of 5RK completely abolished CDO [21]. To explore the possible involvement of S14 phosphorylation in the requirement of 5RK for CDO, we generated a phospho-null version of CSYS-5RK/A, CSYS-5RK/A;S14A (Figure 2A), and subjected cells expressing the mutant to dynamic FRET analysis, in parallel to CSYS;S14A. Strikingly, the FRET ratio reduction of CSYS-5RK/A;S14A in response to hK depolarization was similar to that of CSYS;S14A and consisted of CDO, the fraction that was blocked by Cd (Figure 2C; F(79,3397) = 5.411, *p* < 0.0001, ANOVA with repeated measures). Thus, unlike the case with CSYS, in the

phospho-null mutant intact 5RK is not required for CDO, strongly suggesting that S14 phosphorylation is the molecular determinant responsible for the requirement of 5RK for CDO.
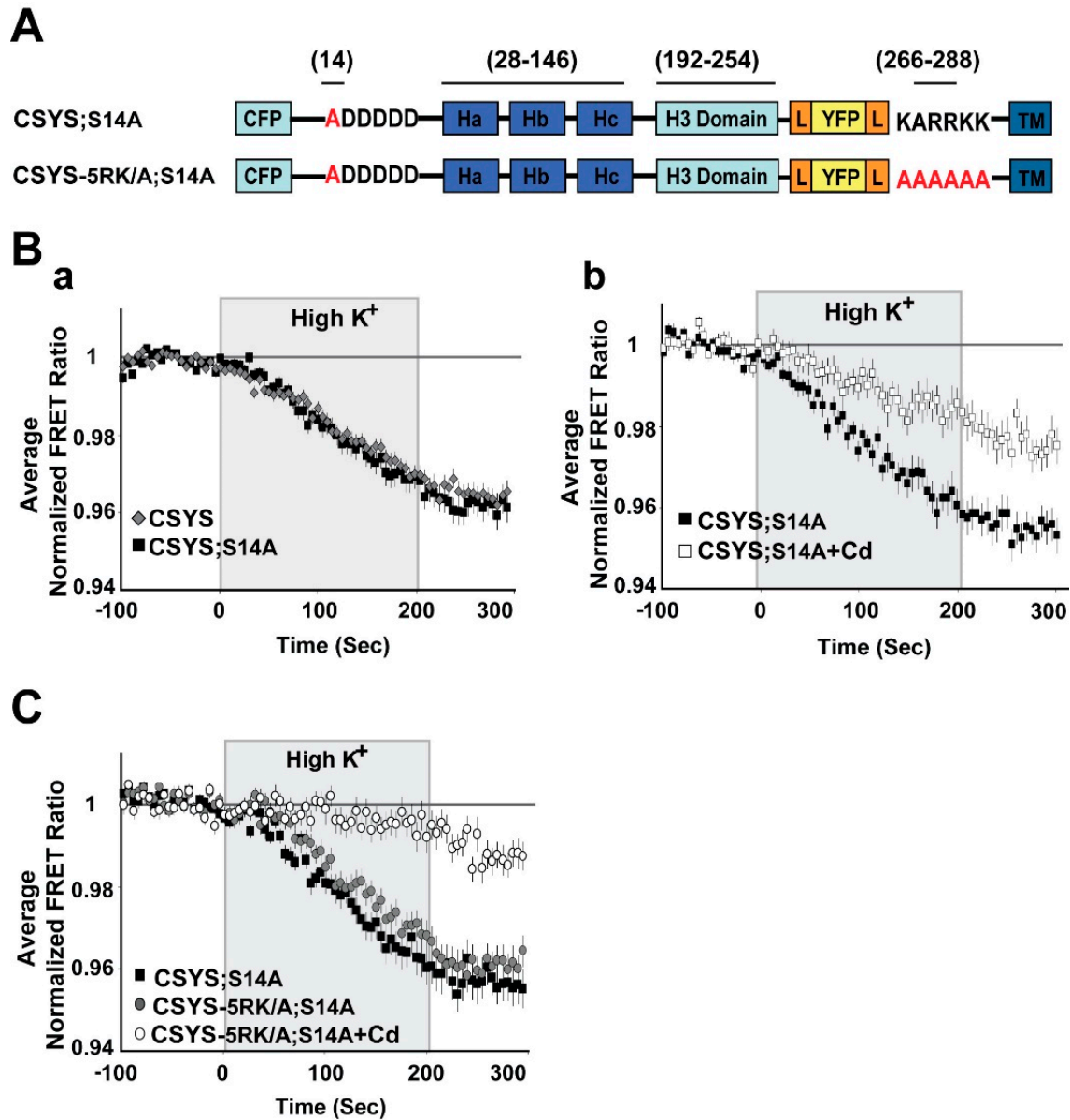

Figure 2. The phospho-null mutant undergoes CDO that does not require intact 5RK. (**A**) Domain structure of the CSYS mutants; CSYS;S14A and CSYS-5RK/A;S14A. Red font highlights important residues (**B**) The phospho-null mutant CSYS;S14A undergoes CDO. (**a**) The reduction in the FRET ratio of the phospho-null mutant CSYS;S14A in response to hK depolarization is similar to that of CSYS (black squares, *n* = 30 cells, and grey diamonds *n* = 32 cells, respectively; 3 experiments). (**b**) Part of the FRET ratio reduction of CSYS;S14A is blocked by Cd and represents CDO. Addition of 200 μM Cd to both control and hK solutions resulted in a smaller reduction in the FRET ratio (white squares, *n* = 22 cells, and black squares, *n* = 26 cells; 2 experiments; $F_{(79,6083)}$ = 15.166, *p* < 0.0001, ANOVA with repeated measures). (**C**) CDO in the phospho-null mutant does not require intact 5RK. Despite the 5RK/A mutation, the reduction in FRET ratio of CSYS-5RK/A;S14A in response to hK depolarization was similar to that of CSYS;S14A (grey circles, *n* = 39, and black squares, *n* = 44, respectively; 5 experiments) and was smaller in the presence of Cd (white circles *n* = 40, 5 experiments; $F_{(79,3397)}$ = 5.411, *p* < 0.0001, ANOVA with repeated measures). Gray background is 200 sec stimulation with high K⁺.

To substantiate this notion, we repeated the same experiments, but with the phospho-mimetic mutation S14E (serine 14 replaced by glutamate). In CSYS;S14E (Figure 3A) the FRET ratio reduction in response to hK depolarization was similar to that of CSYS (Figure 3B(a)), as was the case with CSYS;S14A. However, the neutralization of 5RK in CSYS-5RK/A;S14E (Figure 3A), in contrast to CSYS-5RK/A;S14A, but like in CSYS-5RK/A, caused a significantly smaller FRET ratio reduction (Figure 3B(b); $F_{(79,2844)} = 4.331$, $p < 0.0001$, ANOVA with repeated measures). This suggested that CDO was eliminated in the phospho-mimetic mutant in the absence of intact 5RK, in accord with the notion that it is the S14 phosphorylation that makes 5RK a prerequisite for CDO.
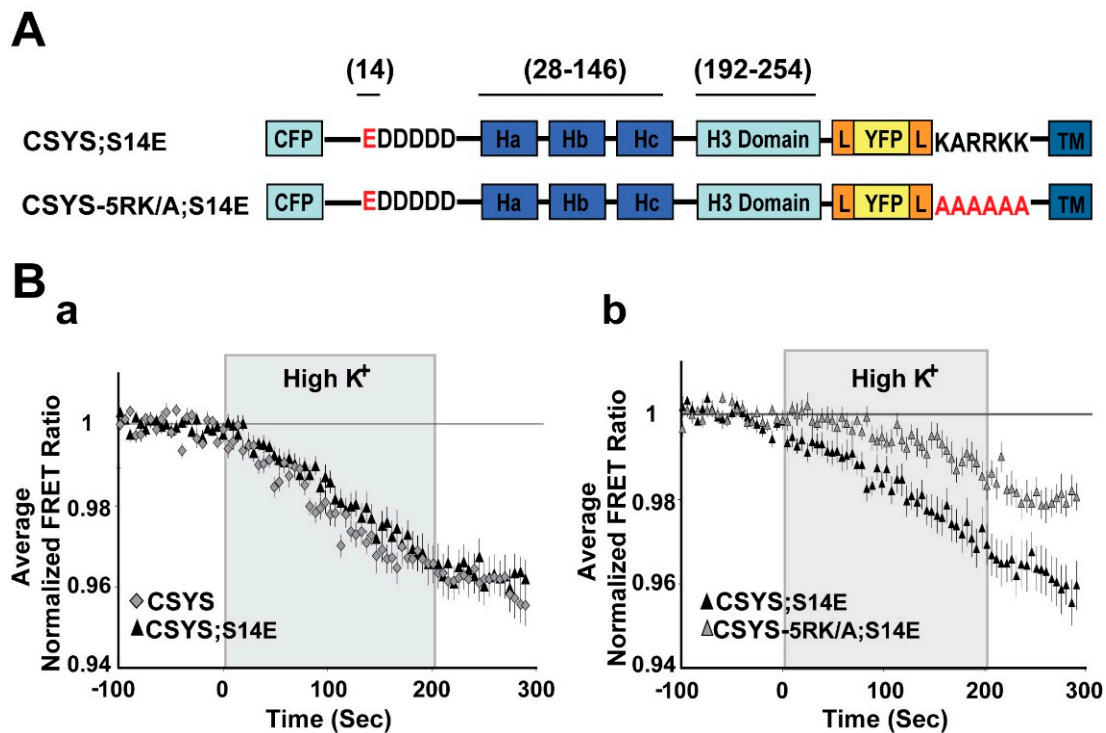

Figure 3. The phospho-mimetic mutant undergoes CDO that requires intact 5RK. (**A**) Domain structure of the phospho-mimetic CSYS mutants, CSYS;S14E and CSYS-5RK/A;S14E. Red font highlights important residues. (**B**) The reduction in the FRET ratio in response to hK depolarization of CSYS;S14E was similar to that of CSYS (**a**); black triangles, *n* = 18, and grey diamonds *n* = 20, respectively; 2 experiments) and included CDO that requires intact 5RK, similarly to CSYS, as it was smaller upon insertion of the 5RK/A mutation (**b**); black triangles *n* = 18, and grey triangles, *n* = 20; 2 experiments; $F_{(79,2844)} = 4.331$, $p < 0.0001$, ANOVA with repeated measures). Gray background is 200 sec stimulation with high K⁺.

As further validation, we chose to test whether elimination of S14 phosphorylation by endogenous CK2 would also eliminate the requirement of 5RK for CDO. We used two approaches to impair endogenous CK2 phosphorylation. First, we targeted the polyacidic N-terminus stretch of Syx (5D), which is a highly-conserved recognition site for CK2 [10]. Dynamic FRET analysis of CSYS-5D/A, with all five aspartates neutralized to alanines (Figure 4A), showed that the FRET ratio reduction in response to hK depolarization was similar to that of CSYS (Figure 4B). However, that of CSYS-5RK/A;5D/A was significantly larger than that of CSYS-5RK/A and was sensitive to Cd blockade (Figure 4C; $F_{(79,5214)} = 5.576$ and $F_{(79,5688)} = 8.959$; respectively, $p < 0.0001$, ANOVA with repeated measures), indicating that the 5RK/A mutation did not eliminate CDO in the 5D/A mutant. This data indicates that prevention of S14 phosphorylation in vivo by abrogating the CK2 recognition site eliminates the requirement of intact 5RK for CDO, essentially mimicking the effect obtained with the S14A mutation.
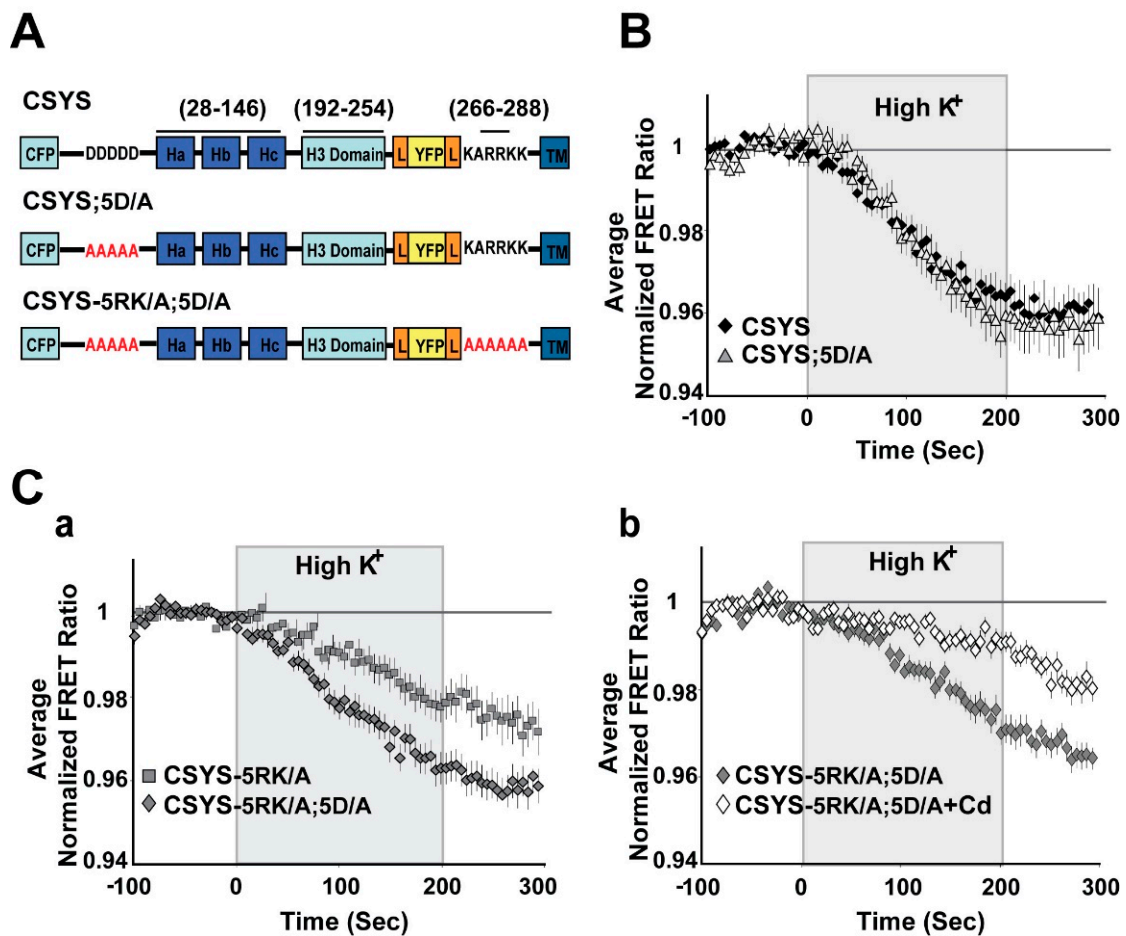
Figure 4. Neutralization of the N-terminal CK2 recognition site in CSYS mimics the effect captured by the phospho-null mutant, eliminating the requirement of 5RK for CDO. (**A**) Domain structures of the CSYS mutants, CSYS;5D/A and CSYS-5RK/A;5D/A. Red font highlights important residues. (**B**) The FRET ratio reduction in response to hK depolarization of CSYS;5D/A was similar to that of CSYS (grey triangles, *n* = 38 and black diamonds, *n* = 65, respectively; 7 experiments). (**C**) The FRET ratio reduction of CSYS-5RK/A;5D/A was larger than that of CSYS-5RK/A (**a**); grey diamonds, *n* = 35, and grey squares *n* = 34, respectively; 7 experiments; F(79,5214) = 5.576, *p* < 0.0001, ANOVA with repeated measures) and was smaller in the presence of Cd, representing CDO that does not require intact 5RK (**b**); white diamond, *n* = 39, and grey diamonds, *n* = 42, respectively; 3 experiments; F(79,5688) = 8.959, *p* < 0.0001, ANOVA with repeated measures).

The second approach to impair the in vivo S14 phosphorylation involved inhibition of CK2 function by tetrabromo-2-benzotriazole (TBB), a highly selective ATP/GTP competitive inhibitor of CK2 [24]. Western blot analysis verified that 20 min incubation of PC12 cells with 20µM TBB, inhibited efficiently phosphorylation of both endogenous Syx and over-expressed CSYS-5RK/A (Figure 5A). Using this approach, we challenged CSYS-5RK/A, which normally does not undergo CDO [21], with the expectation that the prevention of its in vivo phosphorylation by TBB would remove the requirement of 5RK for CDO. Remarkably, incubation with TBB increased the FRET ratio reduction in response to hK depolarization of CSYS-5RK/A, and the effect was Cd-sensitive (Figure 5B; F(79,3239) = 3.239 and F(79,5214) = 3.410; respectively, *p* < 0.0001, ANOVA with repeated measures), indicating that CDO was enabled by the impairment of S14 phosphorylation, as expected.

Taken together, the results derived using the phospho-null (Figure 2) and phospho-mimetic (Figure 3) CSYS mutants with the results of impaired in vivo phosphorylation (Figures 4 and 5), strongly implicate CK2-induced S14 phosphorylation as a regulatory mechanism that imposes absolute dependence on intact 5RK for CDO.
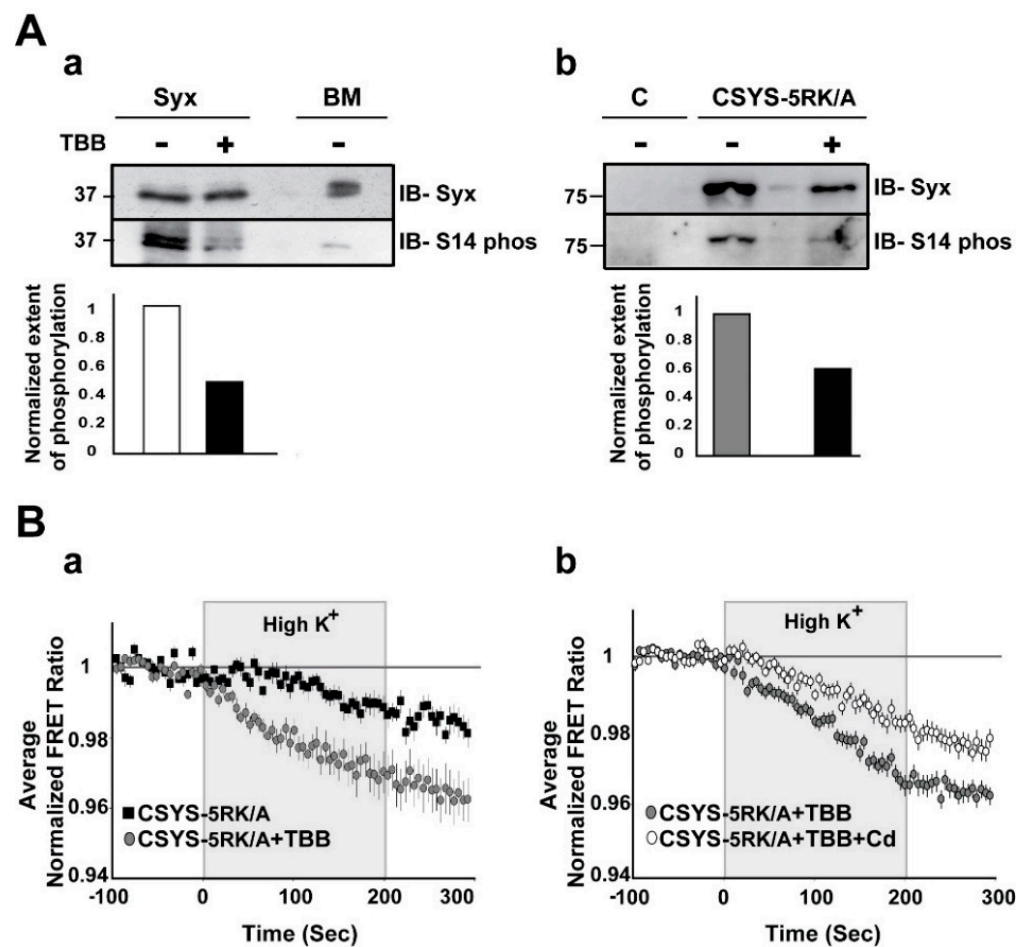
Figure 5. Inhibition of in vivo S14 phosphorylation eliminates the requirement of 5RK for CDO. (**A**) S14 phosphorylation is inhibited by TBB. (**a**) S14 phosphorylation of endogenous Syx in PC12 cells is reduced by TBB. Native Syx was immunoprecipitated with anti-Syx antibody and immunoblotted with either anti-Syx antibody (*IB-Syx*; upper panel) or with Syx S14 phospho-specific antibody (*IB-S14 phos*; middle panel). The extent of phosphorylation (ratio between the corresponding upper and middle intensities) was reduced by TBB (lower panel). Native brain membranes (BM) were loaded as a control. (**b**) S14 phosphorylation of CSYS-5RK/A expressed in PC12 cells is reduced by TBB. CSYS-5RK/A was immunoprecipitated from transfected PC12 cells with anti-YFP antibody and immunoblotted with either anti-Syx antibody (*IB-Syx*; upper panel) or with Syx S14 phospho-specific antibody (*IB-S14 phos;* middle panel). In the presence of TBB the extent of S14 phosphorylation was reduced (lower panel). Molecular weight markers are shown on the left. Native cells were used for control (**c**). (**B**) De-phosphorylation by TBB rescues CDO in CSYS-5RK/A. (**a**) Addition of TBB increased the FRET ratio reduction of cells expressing CSYS-5RK/A in response to hK depolarization (grey circles, *n* = 25, and black squares, *n* = 19; 2 experiments; F(79,3239) = 3.454, *p* < 0.0001, ANOVA with repeated measures) (**b**) In the presence of TBB the FRET ratio reduction was smaller upon addition of Cd (white circles *n* = 34, and grey circles *n* = 34, respectively; 3 experiments; F(79,5214) = 3.410, *p* < 0.0001, ANOVA with repeated measures).

2.2. The Requirement of PIP2 for CDO Is Not Linked to S14 Phosphorylation

Our previous work suggested that CDO is absolutely dependent on PIP2 levels in the PM of PC12 cells [23]. Here, having established the importance of S14 phosphorylation for the requirement of 5RK, we next asked whether phosphorylation could also be linked to the PIP2 requirement. Specifically, we asked whether CDO in the phospho-null mutants, CSYS;S14A and CSYS-5RK/A;S14A, will be eliminated upon hydrolysis of PIP2 by co-expression of the strongly Ca^{2+}-activated phospholipase, Cη2 (PLCη2) [25]. Dynamic

FRET analysis in both mutants revealed that the FRET ratio reductions in response to hK depolarization were significantly smaller in the presence of the mRFP-tagged phospholipase (Figure 6A; $F_{(79,6794)} = 8.167$ and B; $F_{(79,2686)} = 5.343$, $p < 0.0001$, ANOVA with repeated measures); that of CSYS-5RK/A;S14A was verified not to be sensitive to Cd Blockade (Figure 6C), indicating that CDO was eliminated by the phospholipase. Of note, we previously showed that the effect of PLCη2 captured in our experimental system could be fully attributed to its PIP2 hydrolysis function, and not to the generation of secondary messengers [23]. Taken together, in contrast to the requirement of 5RK, the requirement of PIP2 was preserved in the phospho-null mutant, suggesting that it is not conferred by S14 phosphorylation, but rather may reflect an inherent characteristic of CDO.
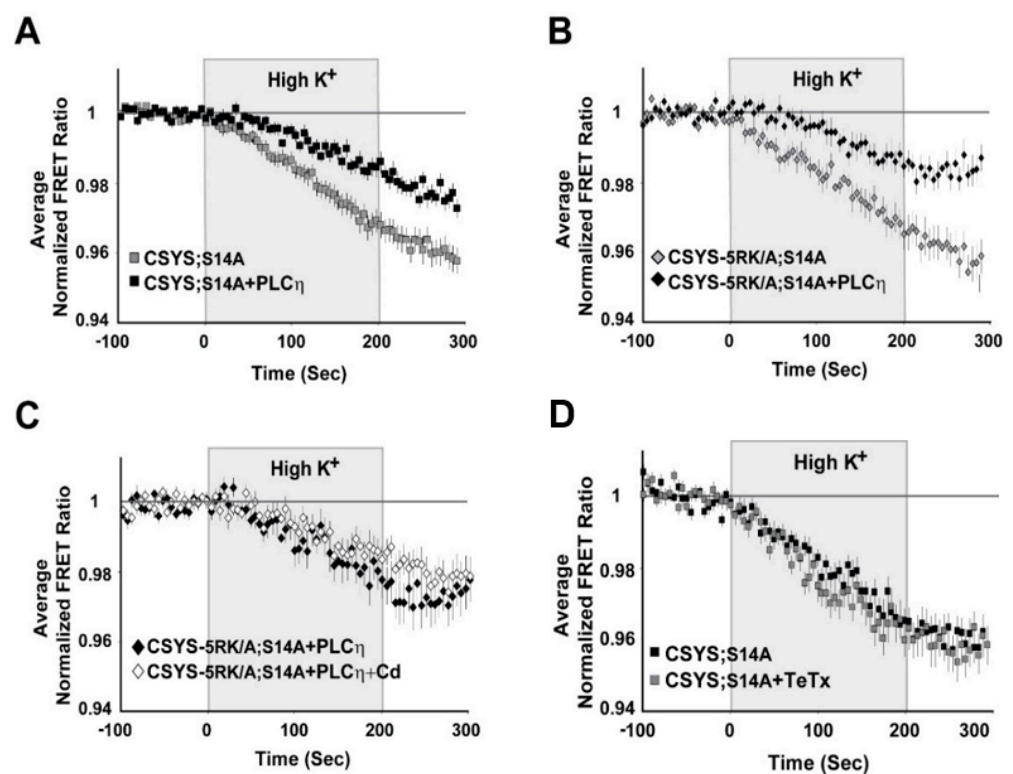

Figure 6. (**A–C**) A requirement for PIP2 is an intrinsic feature of CDO and is independent of S14 phosphorylation. Upon PIP2 hydrolysis by co-expressed PLCη2, the FRET ratio reduction in response to hK depolarization was reduced in cells expressing each of the phospho-null mutants, CSYS;S14A (**A**); grey squares, $n = 50$, and black squares, $n = 42$, respectively; five experiments; $F_{(79,6794)} = 8.167$, $p < 0.0001$, ANOVA with repeated measures) and CSYS-5RK/A;S14A (**B**); black diamonds, $n = 16$ and grey diamonds, $n = 20$, respectively; two experiments; $F_{(79,2686)} = 5.343$, $p < 0.0001$, ANOVA with repeated measures). The FRET ratio reduction of CSYS-5RK/A;S14A in the presence of PLCη2 was insensitive to the addition of Cd, indicating that PLCη2 inhibited CDO (**C**); white diamonds, $n = 21$ and black diamonds, $n = 23$, respectively; two experiments). (**D**) The conformational transition of the CSYS phospho-null mutant does not involve Syb2. Syb2 cleavage by TeTx-LC did not have any effect on the FRET ratio reduction in response to hK depolarization of CSYS;S14A (black squares, $n = 23$ and grey squares, $n = 20$, respectively; three experiments).

2.3. S14 Phosphorylation Is Required for CDO to Occur within a Vesicular Context

Having recognized the significance of S14 phosphorylation for CDO, the next step was to understand its relevance to vesicle release. Previously, we have shown that CSYS, which is constitutively S14 phosphorylated in vivo (see Figure 1B), undergoes CDO that occurs in a vesicular context, as it was eliminated following 4 h incubation with 30 nM light chain of tetanus toxin (TeTx LC), which cleaves the vesicular SNARE Syb2 [23]. Here, we examined whether the CDO of the phospho-null mutant, CSYS;S14A, also involves

Syb2. Strikingly, in contrast to intact CSYS, there was no effect of TeTx LC on the FRET ratio reduction in response to hK in the phospho-null mutant (Figure 6D), indicating that its opening, including CDO, does not involve intact Syb2, possibly occurring within a release-irrelevant environment.

2.4. S14 Phosphorylation Is Required for Ca^{2+}-Triggered Release and for Enhanced Spontaneous Release Conferred by the 5RK/A Mutation

Previously, an amperometric analysis of catecholamine release showed that 5RK plays a central role in clamping spontaneous release and promoting Ca^{2+}-triggered release in PC12 cells, as the 5RK/A mutation enhanced spontaneous release and inhibited Ca^{2+}-triggered release [23]. To assess the relevance of S14 phosphorylation to secretion directly, we used carbon fiber amperometry to analyze the secretion phenotype of the phospho-null mutant CSYS;S14A and compared it with the, previously characterized [23], phenotype of CSYS. In order to reduce potentially confounding effects from endogenous Syx, we used cells transfected with the light chain of BoNT-C1α51 (BoNT-C1), which spares SNAP-25 cleavage and cleaves only endogenous Syx [26], precluding Syx from mediating membrane fusion [27]. We have previously shown that CSYS(R), a CSYS mutant bearing the K253I mutation, which confers resistance to BoNT-C1 [14], is indeed resistant to the co-expressed toxin and retains its PM expression in PC12 cells. Importantly, CSYS(R) was shown to rescue the inhibition of exocytosis by the toxin, in both PC12 cells [21] and in hippocampal neurons [22]. Accordingly, we generated here the toxin resistant version of the phospho-null mutant, CSYS;S14A(R), and verified that it is resistant to the toxin and is expressed on the PM of cells co-expressing the toxin (Figure 7A). Comparative amperometric measurements, 1 min before (to detect spontaneous events) and 1 min after a 10 sec application of hK solution (to detect evoked events), performed in cells co-expressing the toxin with CSYS;S14A(R) or CSYS(R) in the same experiments, revealed that cells expressing either construct had few spontaneous release events (Figure 7B). Notably, in contrast to CSYS(R), which exhibited evoked release in response to hK depolarization, there was no significant change in the release pattern of CSYS;S14A(R) expressing cells in response to hK depolarization, neither in number of spikes or total charge release (Figure 7B,C), indicating that the phospho-null mutation eliminated evoked release. Furthermore, cells expressing the toxin resistant version of the phospho-null CSYS-5RK/A mutant, CSYS-5RKA;S14A(R), did not display enhanced spontaneous release (Figure 7D), as was observed in cells expressing CSYS-5RK/A(R) [23]; namely, the phospho-null mutation eliminated also the enhanced spontaneous release conferred by the 5RK/A mutation.

Together, the amperometry analysis (Figure 7) and the FRET analysis of the TeTx effect (Figure 6D), indicate that S14 phosphorylation is required for Ca^{2+}-triggered release and for enhanced spontaneous release conferred by the 5RK/A mutation.
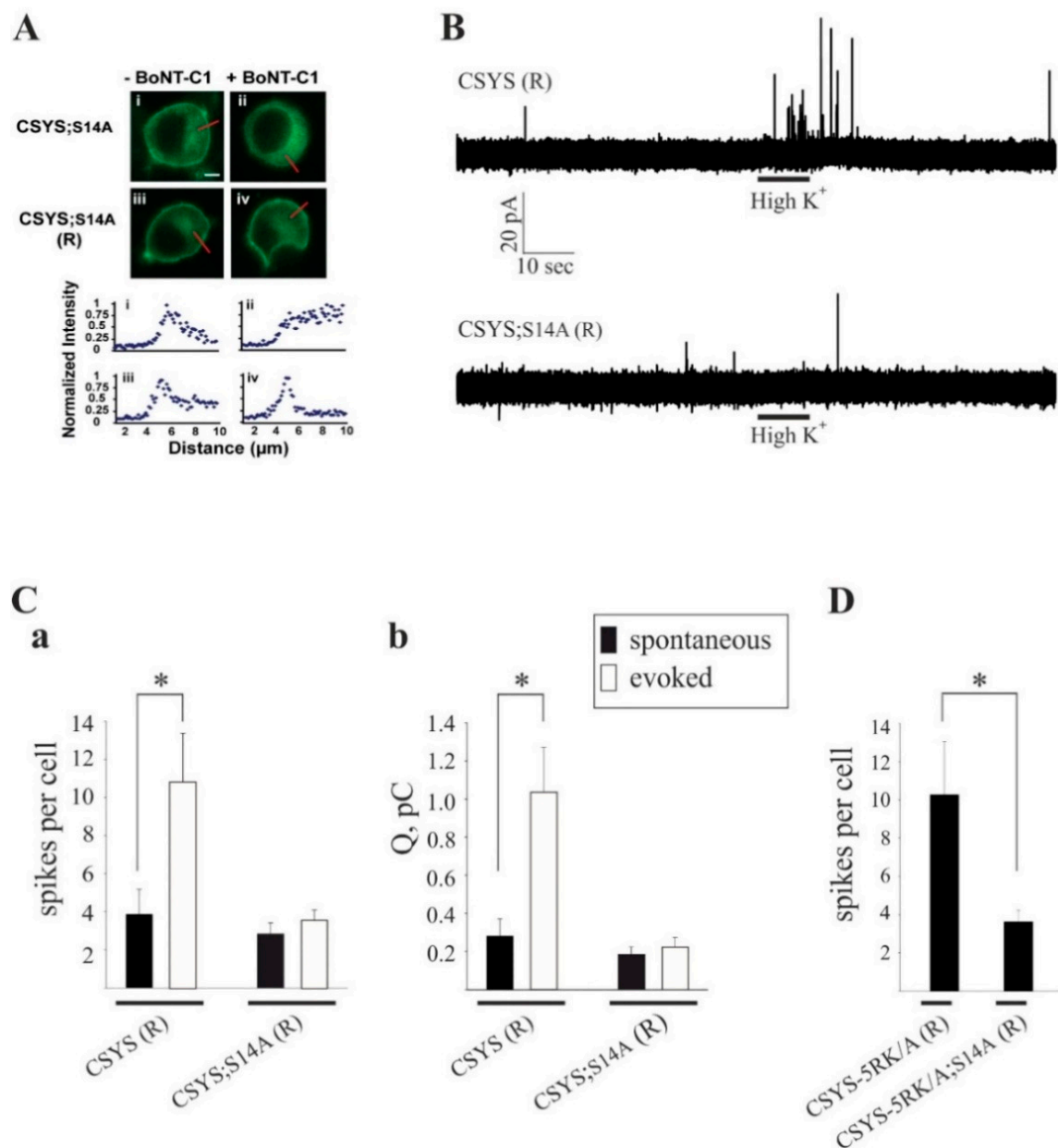
Figure 7. The phospho-null mutation abolishes Ca^{2+}-triggered release and the enhanced spontaneous release conferred by the 5RK/A mutation. (**A**) CSYS;S14A (R), bearing the K253I mutation, is located in the PM region of PC12 cells and is resistant to cleavage by BoNT-C1. *Upper panel*: confocal images of PC12 cells demonstrating that CSYS;S14A (R) (iii) retained its PM distribution upon BoNT-C1 co-expression (iv), indicating its resistance to BoNT-C1, while CSYS;S14A (i) was located in the cytosol upon BoNT-C1 co-expression (ii). Scale bar: 5 mm. *Lower panel:* normalized fluorescence intensity profiles of the above cells indicating PM or cytosolic expression. The fluorescence profiles were determined from line scans (red lines, upper panel) taken from the outside to the middle of each cell. (**B**) Representative amperometric recordings of catecholamine release from cells transfected CSYS (R) or with CSYS;S14A (R), before and after hK depolarization. (**C**) Average number of spikes (**a**) and total charge release (**b**) for spontaneous (before hK) and evoked (after hK) release from PC12 cells co-transfected with BoNT-C and either CSYS (R) or CSYS;S14A (R) ($t(14) = 2.16$, * $p = 0.048$ (**a**) and $t(14) = 2.84$, * $p = 0.013$ (**b**), paired t-test). (**D**) Average number of spikes for spontaneous release from PC12 cells co-transfected with BoNT-C and either CSYS-5RK/A (R) or CSYS-5RK/A;S14A (R) ($n = 11$ and 8, respectively, * $p = 0.044$, Mann-Whitney Rank Sum test).

3. Discussion

This study demonstrates the importance of CK2 phosphorylation of Syx at S14 in the regulation of a depolarization-induced Ca^{2+}-dependent opening of Syx, and in Ca^{2+}-triggered release. The role of S14 phosphorylation is highlighted by three major findings obtained using the Syx-based FRET probe, CSYS, previously shown to support Ca^{2+}-triggered release [21,23]. The first finding was obtained by dynamic FRET analysis of the effects of phospho-null and phospho-mimetic CSYS mutations, as well as the effect of impaired in vivo *S14* phosphorylation, either by disruption of the CK2 recognition site or inhibition of the catalytic site. These experiments establish that S14 phosphorylation is responsible for the previously described [21] requirement of the juxtamembrane 5RK stretch of Syx for CDO. The second finding, obtained by dynamic FRET analysis of the effect of the phospho-null mutation in the presence of TeTx LC, which cleaves the vesicular SNARE Syb, reveals that S14 phosphorylation causes CDO to be dependent on intact Syb2, possibly occurring within a vesicular context. The third finding, obtained by amperometric analysis of the effects of the phospho-null mutation on secretion phenotypes, shows that S14 phosphorylation is required for release, spontaneous and Ca^{2+}-triggered. These findings demonstrate that S14 phosphorylation is crucial for Syx functioning within a vesicular context under the control of 5RK to support Ca^{2+}-dependent release. Although PC12 cells are derived from rat, the universality of secretion mechanisms allows us to hypothesize that similar phenomena are expected in other mammals. Together with our previous results, which assigned a dual role for 5RK in clamping spontaneous release and stimulating Ca^{2+}-triggered release [23], these findings provide a basis for a mechanistic model (described below) that describes interrelated roles for S14 phosphorylation and 5RK in the functioning of Syx in Ca^{2+}-dependent exocytosis.

It should be noted that, although several proteins involved in Ca^{2+}-dependent exocytosis, including Syt-1, Syx, VAMP-2, and CAPS, are in vitro substrates of CK2, [28–31], only the activity of CAPS has so far been shown to be dependent on CK2 phosphorylation in vivo. This study is the first report to directly link in vivo CK2 phosphorylation and the activity of Syx as important for exocytosis.

Model Describing the Interrelated Roles of CK2-Induced S14 Phosphorylation and 5RK in the Functioning of Syx in Ca^{2+}-Triggered Release

Integrating our FRET and amperometric results, previous [21,23] and current, together with evidence from the recent literature, has allowed us to formulate a number of postulations that provide the basis for a model of Syx functioning in exocytosis (Figure 8).

First, in spite of the documented importance of the electrostatic interactions between PIP2 and 5RK in vesicle exocytosis (Introduction; reviewed in [32]), the interaction between PIP2 and Syx identified in our study proved to be unrelated to 5RK. We demonstrated that, while PIP2 is essential for CDO in both the S14 phosphorylated [23] and the non-phosphorylated (Figure 6) states of CSYS, 5RK is essential for CDO only in the phosphorylated state ([23] and Figures 2–5). This means that the roles of 5RK and PIP2 in CDO are distinct and do not involve the commonly assumed PIP2-5RK electrostatic interaction. Indeed, molecular dynamics simulations suggested that sites in Syx that are critical to its interaction with PIP2 are not confined to 5RK; in the closed conformation of Syx, the N terminus presumably lies in a juxtamembrane position that enables it to interact with PIP2 [33]. Taken together, *the first postulation is that an inherent PIP2-Syx interaction, possibly involving the N terminus of Syx, is absolutely required for CDO, regardless of CK2 phosphorylation.*

Second, we note that CK2 phosphorylation has been reported to play a significant role in neuronal excitability in a location-specific manner. Specifically, CK2 phosphorylation has been shown to regulate the accumulation of voltage gated Na^+ [34,35] and K^+ [36,37] channels at the axon initial segment, with great impact on axonal excitability, and to affect NMDA receptors in a receptor-location-specific manner to modulate long term potentiation [38]. Notably, location-specificity was reported also for S14 phosphorylated Syx, shown to localize to discrete domains along a subset of axons [12]. Here we show

that, in contrast to CSYS (being endogenously S14 phosphorylated; Figure 1B(b)), the phospho-null CSYS mutant undergoes CDO that does not involve the vesicular SNARE, Syb2 (Figure 6D) and does not support Ca^{2+}-triggered release (Figure 7A–C). Furthermore, in contrast to CSYS-5RK/A (being endogenously S14 phosphorylated; Figure 5A(b)), the phospho-null CSYS-5RK/A mutant does not exhibit prominent spontaneous release (Figure 7D). These observations allow us to associate the determined location-specificity of S14 phosphorylated Syx with release-competent sites, where Syx acts to support vesicle release events, spontaneous and Ca^{2+}-triggered. Thus, *the second postulation is that S14 phosphorylated Syx is specific to release-competent sites. In these sites Syx can be engaged in ternary SNARE complex assembly and support release.*
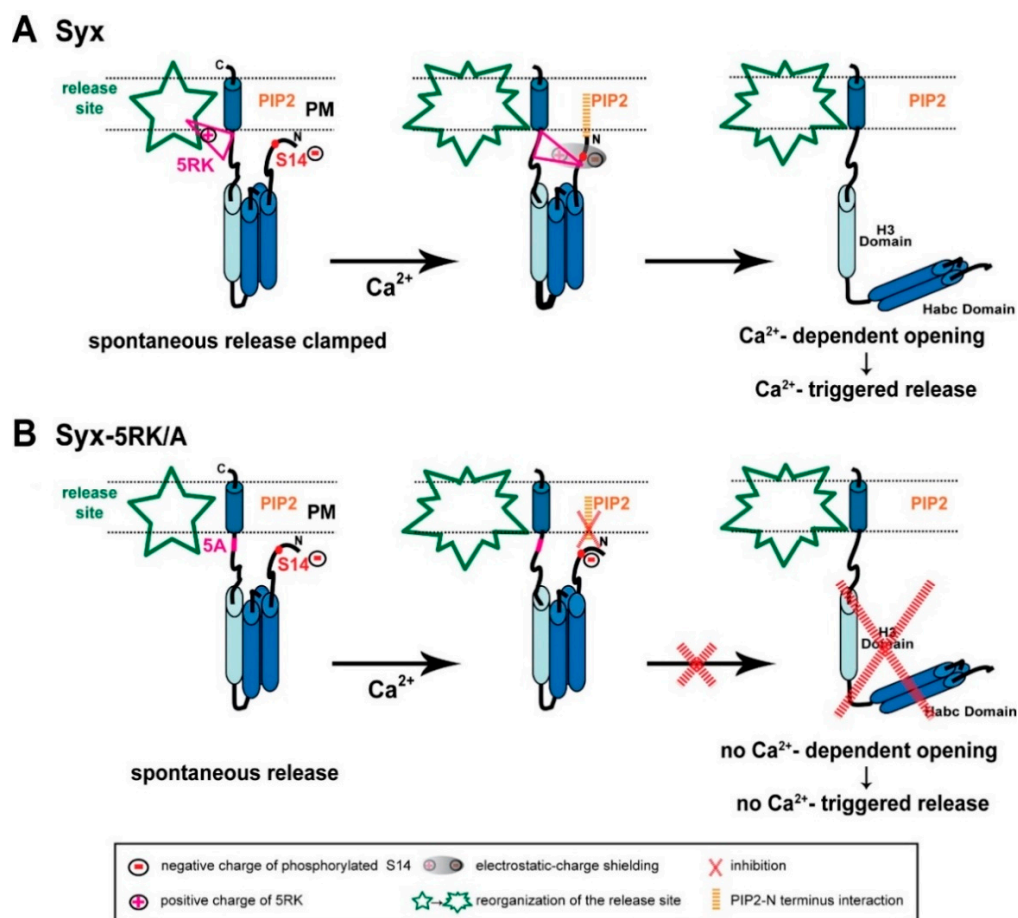

Figure 8. Model of the interrelated roles of 5RK and S14 phosphorylation in Syx functioning during exocytosis. (**A**) *Left panel,* Syx (blue cylinders) maintains the closed conformation at release competent sites (green; release site) due to S14 phosphorylation by CK2. Prior to Ca^{2+} entry, 5RK (pink triangle) interacts with certain lipids and/or fusogenic proteins that enable 5RK to act as a fusion clamp that inhibits spontaneous release. Under these conditions, PIP2 is not likely to interact with Syx (possibly with the N terminus), because of hindrance by the negative charge of the phosphate group of phosphorylated S14. *Middle and right panels*, Sequential reactions in response to depolarization-induced intracellular Ca^{2+} elevation start with reorganization of the release site and an intramolecular rearrangement of Syx that draws the positive charges of 5RK and the negative charges of phosphorylated S14 into close proximity, resulting in electrostatic-charge shielding (grey shade) of the phosphate group (*middle*). The consequent formation of the PIP2–Syx interaction (orange) enables Syx to undergo CDO and to promote Ca^{2+}-triggered release (*right*). (**B**) *Left panel,* the S14-phosphorylated 5RK/A mutant lacks the 5RK clamp and exhibits enhanced spontaneous release. *Middle and right panels,* In response to depolarization-induced intracellular Ca^{2+} elevation there is no charge shielding of the phosphate group so that PIP2 cannot interact with Syx, consequently Syx cannot undergo CDO and promote Ca^{2+}-triggered release. (PM; plasma membrane).

Third, the previously described secretion phenotype of CSYS-5RK/A, with enhanced spontaneous release, suggested that 5RK serves as a fusion clamp [23]. Thus, *the third postulation is that 5RK acts to clamp spontaneous release at release-competent sites,* presumably via its well documented interactions with lipids and/or fusogenic proteins (*Introduction*).

Fourth, since CSYS-5RK/A cannot undergo CDO [21], unless phosphorylation of its S14 is impaired (Figures 2C and 5B), *the fourth postulation is that S14 phosphorylation inhibits CDO in the absence of intact 5RK; 5RK relieves the inhibition*, as exemplified in CSYS (with intact 5RK), which undergoes CDO while being phosphorylated. We hypothesize that the mechanism underlying the inhibition is the formation of an electrostatic repulsion between the negatively charged phosphate group of phosphorylated S14 and PIP2, interfering with the N-terminal-PIP2 interaction that is essential for the ability of Syx to undergo CDO (first postulation). This inhibition can be relieved upon masking of the negative charge of the phosphate moiety by the positive charge of 5RK (both charges presumably lie in juxtamembrane positions). The charge masking may require Ca^{2+}-induced structural reorganization(s) of Syx, possibly with respect to the phospholipid environment (for example see: [39]), that bring 5RK and the phosphate moiety into close proximity with consequent electrostatic-charge shielding.

Fifth, since Ca^2-triggered release, similarly to CDO, is induced only in the presence of 5RK, our fifth postulation is that the relief by 5RK of S14 phosphorylation-induced inhibition of CDO (fourth postulation) underlies Ca^{2+}-triggered release.

Based on the above postulations, we present the following model of interrelated roles of 5RK and S14 phosphorylation in Syx functioning during exocytosis (Figure 8A). S14 phosphorylated Syx, in contrast to its non-phosphorylated form (not shown in the model; see below), resides in release-competent sites. Prior to Ca^{2+} entry, Syx assumes its closed conformation, with 5RK serving as a fusion clamp that inhibits spontaneous release, possibly via interactions with phospholipids and/or fusogenic proteins (Figure 8A, left). In response to a depolarization-induced intracellular elevation of Ca^{2+}, an intramolecular rearrangement of Syx, possibly associated with the reorganization of the release-competent site, draws 5RK and phosphorylated S14 into close proximity. The resulting electrostatic-charge shielding of the phosphate group by 5RK permits an otherwise inhibited interaction of the N terminus of Syx with PIP2, which is essential for CDO (Figure 8A, middle). Subsequently, Syx undergoes CDO and promotes Ca^{2+}-triggered release (Figure 8A, right). In contrast, the 5RK/A mutation of Syx (Figure 8B) enhances spontaneous release, due to lack of the 5RK fusion clamp (Figure 8B, left), while Ca^{2+}-triggered release is inhibited, because the PIP2-Syx interaction, which enables CDO, cannot occur while the phosphate charge is not masked by 5RK (Figure 8B, middle & right).

In conclusion, we suggest that CK2-induced S14 phosphorylation of Syx is essential for vesicle release as it localizes Syx to a release-relevant setting in which it acts in concert with 5RK to make release dependent on depolarization-induced intracellular Ca^{2+} elevation.

According to our paradigm, non-phosphorylated Syx (not shown in the model) is miss-located to a release-irrelevant environment. There, it undergoes CDO that does not include Syb2 (Figure 6D), likely reflecting the formation of Ca^{2+}-induced non-productive SNARE intermediate(s) (e.g., 2:1 Syx/SNAP-25 binary complexes [15,40], and does not support vesicle fusion (Figure 7). Notably, in the absence of S14 phosphorylation, there is no electrostatic repulsion between the N terminus and PIP2 so that CDO can occur regardless of whether intact 5RK is present (Figure 2). Namely, CDO regulation by 5RK is confined to release-relevant sites.

4. Materials and Methods

4.1. Plasmid Construction

Double-labeled Syx (CSYS) and CSYS-5RK/A cDNA were generated as described in [21]. CSYS;S14A was generated by introducing a point mutation, S14A, in the N-peptide domain of CSYS. CSYS;5D/A was generated by introducing five point mutations, D15,16,17,18,19A, in the N-peptide domain of CSYS. The BoNT-C1-resistant mutation

(CSYS(R)) was generated by introducing one point mutation, K253I, in the BoNT-C1 recognizing sequence [41]. For PC12 transfection, the constructs were cloned into pcDNA3 vector using EcoRI and XbaI restriction sites. The PLCη2 construct was kindly provided by T.F.J. Martin (University of Wisconsin-Madison, Madison, WI, USA). BoNT-C1α51 was subcloned into an mRFP pcDNA3 vector containing an internal ribosome entry site (IRES).

4.2. PC12 Cells Preparation and Transfection for FRET Experiments

PC12 cells (ATCC CRL-1721) were maintained at 37 °C/5% CO_2 in Dulbecco's Modified Eagle's Medium (DMEM) with high glucose (Sigma-Aldrich Israel, Rehovot, Israel) supplemented with 10% bovine serum, 5% L-glutamine, 100 U/mL penicillin, and 0.1 mg/mL streptomycin. For imaging, cells were replated to ~60% confluence on poly-L-lysine (Sigma-Aldrich) coated 35 mm glass bottom culture dishes, and allowed to adhere overnight. Cells were transfected with 1.5 μg of the CSYS mutation probes, using Lipofectamine 2000 (Invitrogen, Watham, MA USA). Imaging experiments were conducted at room temperature, 24 h after transfection. During the experiment, the transfected cells were superfused through a 2 mL bath, with physiological (2.8 mM K^+) and high K^+ (105 mM K^+) solutions as described previously [42].

4.3. Dynamic FRET Assay

PC12 cells were imaged using the Zeiss 510 Meta confocal microscope (Karl Zeiss AG, Jena, Germany) with a C-Apochromat $40\times/1.2$ NA water objective and excited with a 405-nm laser every 5 s for a total of 400 s. During the sequential imaging, the cells were imaged in a control, 2.8 mM K^+, solution for 100 s, before and after 200 s of 105 mM high K^+ solution, for a total imaging time of 400 s. Fluorescent signals were collected with a 510META confocal microscope (Zeiss, Jena, Germany) using its "channel mode". Cells were excited with a 405 nm laser band and the emission was filtered through the main beam splitter HFT405/514/633 nm and further separated by a secondary beam splitter, NFT515 nm. CFP and YFP fluorescence were collected by a 470–500 nm and 505–550 nm band pass filter, respectively, and directed into two separate photomultipliers. Under these settings, the leak of YFP into the CFP recording window is purely optical, and very low (<1%) [43], and remains constant regardless of changes in FRET, thus it does not require any corrections. YFP and CFP intensities in a region of interest (ROI) on the cell membrane were calculated, and background fluorescence was quantified from an ROI defined in each image in an area containing no fluorescent cells. The background-subtracted fluorescence intensity at each exposure time point was normalized to the average of the initial measurements in each cell (before the high K^+ solution was added). The FRET ratio of normalized intensities was denoted as F_{YFP}/F_{CFP}. Changes in FRET are reflected as changes in the FRET ratio.

4.4. Cell Culture for the Amperometry Experiments

PC12 cells were obtained from the American Type Culture Collection (ATCC, Rockville, MD, USA), and maintained in RPMI-1640 media supplemented with 10% heat-inactivated horse serum and 5% fetal bovine serum (Sigma-Aldrich Israel, Rehovot), in a 7% CO_2 atmosphere at 37 °C. The cells were grown on mouse collagen IV-coated flasks (Becton Dickinson, Bedford, MA, USA) and were subcultured approximately every 7 days. Cells were transfected using Lipofectamine-2000 (Invitrogen, Watham, MA USA).

4.5. Amperometry Measurements

Amperometric currents were recorded with a VA-10 amplifier (npi Electronics GmbH, Tamm, Germany). A constant voltage of +700 mV was applied to the 5 μm OD carbon electrode (ALA Scientific, Westbury, NY, USA). The currents were filtered at 1 kHz and digitized at 10 kHz using a Digidata 1322A analog-to-digital converter and the Clampex 9 software package (Axon CNS Molecular Devices, Sunnyvale, CA, USA). Data were analyzed by the customized macro for IGOR PRO software [44]. Spikes smaller than 5 pA were considered to be noise and were discarded. The bath solution contained (in mM): 150

NaCl, 5 KCl, 1.2 MgCl$_2$, 5 glucose, 10 Hepes, 2 CaCl$_2$, pH 7.4, and the high K$^+$ solution contained (in mM): 100 KCl, 50 CaCl$_2$, 0.7 MgCl$_2$, Hepes 10, pH 7.4. Similarly to what was shown in chromaffin cells [45], we observed reduced spontaneous release in the presence of elevated [Ca^{2+}] in PC12 cells (data not shown); therefore, spontaneous events were monitored in physiological [Ca^{2+}] (2 mM).

4.6. Immunoprecipitation (IP) and Immunoblotting (IB) in PC12 Cells

PC12 cells were homogenized in the lysis buffer: 150 mM NaCl; 50 mM Tris-HCl; 5 mM EDTA; 1 mM EGTA; 10 mM sodium fluoride and 1 mM sodium orthovanadate, containing a cocktail of protease inhibitors (Promega, Madison WI USA). Following solubilization by 1% Triton X-100, the homogenate was centrifuged (12,000× g/25 min/4 °C) and the supernatant was incubated with YFP (MBS 833304) antibody overnight. Proteins bound to the beads were eluted by heating at 95 °C, for 4 min in the SDS-PAGE sample loading buffer. Immunoprecipitated proteins were separated by SDS-PAGE and subjected to Western blotting with antibody against S14 phosphorylated Syx (ab63571; Abcam, Cambridge UK), using the ECL detection system (Pierce Protein Research Products, Thermo Scientific, Waltham, MA USA). In experiments investigating the effect of TBB, cells were incubated with 20 μM of TBB (Merck group, St. Louis MO USA) for one hour prior to homogenization.

4.7. Immunoprecipitation (IP) and Immunoblotting (IB) in Xenopus Oocytes

De-folliculated *Xenopus* oocytes were metabolically labeled 4 h after mRNA injection, by incubation in NDE solution containing 0.3 mCi/mL of ^{35}[S] methionine/cysteine for 2 days. After this time, six to eight oocytes were homogenized in 1 mL of medium composed of 20 mM Tris (pH 7.4), 5 mM EDTA, 5 mM EGTA, and 100 mM NaCl [containing protease inhibitor cocktail (Roche, Indianapolis, IN USA)]. Debris was removed by centrifugation for 10 min at 4 °C. After solubilization by 1% Triton X-100, the homogenate was centrifuged (12,000× g/15 min/4 °C) and the supernatants were incubated with anti-Syx antibody (Alomone labs, Jerusalem Israel) overnight at 4 °C with gentle rotation. Immunoprecipitated proteins were separated by SDS-PAGE and subjected to Western blotting with antibody against Syx phospho-S14 (ab63571; Abcam, Cambridge UK). Digitized scans were derived by PhosphorImager (Molecular Dynamics, Eugene, OR, USA) and relative intensities were quantitated by ImageQuant.

4.8. Experimental Design and Statistical Analysis

Experiments with adult female *Xenopus laevis* frogs were approved by Tel Aviv University Institutional Animal Care and Use Committee (permits # 01–16-104 and 01–20-083). Data was summarized as means ± S.E.M. The number of samples (n) indicates the number of cells per group. Statistical analysis was performed in either SPSS v24 (IBM, Israel, Petach Tikva) or SigmaPlot v11 (Systat Software, Chicago, IL USA). One-way analysis of variance (ANOVA) for repeated measures was used to analyze time course FRET (dynamic FRET) experiments. For amperometry experiments where events were monitored before and after stimulation in each cell, paired t-test analysis was used. For 2 independent groups of events with non-Gaussian distributions, we used the Mann-Whitney Rank Sum Test. Multiple groups were compared by ANOVA followed by post-hoc Tukey's test. Asterisks in the figures indicate statistically significant differences as follows: * $p < 0.05$; ** $p < 0.001$.

Author Contributions: N.B.-B., D.S.-L. and D.C. performed the experiments. I.L., N.B.-B. and D.S.-L. conceived and wrote the paper. All authors have read and agreed to the published version of the manuscript.

Institutional Review Board Statement: Not applicable.

Informed Consent Statement: Not applicable.

Data Availability Statement: Data supporting results can be found in: bioRxiv 2020.08.20.258863; doi:https://doi.org/10.1101/2020.08.20.258863.

Conflicts of Interest: The authors declare no conflict of interest.

References

1. Rizo, J.; Xu, J. The synaptic vesicle release machinery. *Annu. Rev. Biophys* **2015**, *44*, 339–367. [CrossRef] [PubMed]
2. Rothman, J.E. The protein machinery of vesicle budding and fusion. *Protein Sci.* **1996**, *5*, 185–194. [CrossRef] [PubMed]
3. Fernandez, I.; Ubach, J.; Dulubova, I.; Zhang, X.; Sudhof, T.C.; Rizo, J. Three-dimensional structure of an evolutionarily conserved N-terminal domain of syntaxin 1A. *Cell* **1998**, *94*, 841–849. [CrossRef]
4. Dulubova, I.; Khvotchev, M.; Liu, S.; Huryeva, I.; Sudhof, T.C.; Rizo, J. Munc18-1 binds directly to the neuronal SNARE complex. *Proc. Natl. Acad. Sci. USA* **2007**, *104*, 2697–2702. [CrossRef]
5. Rickman, C.; Medine, C.N.; Bergmann, A.; Duncan, R.R. Functionally and spatially distinct modes of munc18-syntaxin 1 interaction. *J. Biol. Chem.* **2007**, *282*, 12097–12103. [CrossRef]
6. Deak, F.; Xu, Y.; Chang, W.P.; Dulubova, I.; Khvotchev, M.; Liu, X.; Sudhof, T.C.; Rizo, J. Munc18-1 binding to the neuronal SNARE complex controls synaptic vesicle priming. *J. Cell Biol.* **2009**, *184*, 751–764. [CrossRef] [PubMed]
7. Khvotchev, M.; Dulubova, I.; Sun, J.; Dai, H.; Rizo, J.; Sudhof, T.C. Dual modes of Munc18-1/SNARE interactions are coupled by functionally critical binding to syntaxin-1 N terminus. *J. Neurosci.* **2007**, *27*, 12147–12155. [CrossRef] [PubMed]
8. Rathore, S.S.; Bend, E.G.; Yu, H.; Hammarlund, M.; Jorgensen, E.M.; Shen, J. Syntaxin N-terminal peptide motif is an initiation factor for the assembly of the SNARE-Sec1/Munc18 membrane fusion complex. *Proc. Natl. Acad. Sci. USA* **2010**, *107*, 22399–22406. [CrossRef]
9. Dubois, T.; Kerai, P.; Learmonth, M.; Cronshaw, A.; Aitken, A. Identification of syntaxin-1A sites of phosphorylation by casein kinase I and casein kinase II. *Eur. J. Biochem.* **2002**, *269*, 909–914. [CrossRef]
10. Rickman, C.; Duncan, R.R. Munc18/Syntaxin interaction kinetics control secretory vesicle dynamics. *J. Biol. Chem.* **2010**, *285*, 3965–3972. [CrossRef]
11. Cozza, G.; Pinna, L.A.; Moro, S. Protein kinase CK2 inhibitors: A patent review. *Expert Opin. Ther. Pat.* **2012**, *22*, 1081–1097. [CrossRef] [PubMed]
12. Foletti, D.L.; Lin, R.; Finley, M.A.; Scheller, R.H. Phosphorylated syntaxin 1 is localized to discrete domains along a subset of axons. *J. Neurosci.* **2000**, *20*, 4535–4544. [CrossRef]
13. Risinger, C.; Bennett, M.K. Differential phosphorylation of syntaxin and synaptosome-associated protein of 25 kDa (SNAP-25) isoforms. *J. Neurochem.* **1999**, *72*, 614–624. [CrossRef]
14. Lam, A.D.; Tryoen-Toth, P.; Tsai, B.; Vitale, N.; Stuenkel, E.L. SNARE-catalyzed fusion events are regulated by Syntaxin1A-lipid interactions. *Mol. Biol. Cell* **2008**, *19*, 485–497. [CrossRef] [PubMed]
15. Hernandez, J.M.; Stein, A.; Behrmann, E.; Riedel, D.; Cypionka, A.; Farsi, Z.; Walla, P.J.; Raunser, S.; Jahn, R. Membrane fusion intermediates via directional and full assembly of the SNARE complex. *Science* **2012**, *336*, 1581–1584. [CrossRef]
16. James, D.J.; Kowalchyk, J.; Daily, N.; Petrie, M.; Martin, T.F. CAPS drives trans-SNARE complex formation and membrane fusion through syntaxin interactions. *Proc. Natl. Acad. Sci. USA* **2009**, *106*, 17308–17313. [CrossRef] [PubMed]
17. Murray, D.H.; Tamm, L.K. Clustering of syntaxin-1A in model membranes is modulated by phosphatidylinositol 4,5-bisphosphate and cholesterol. *Biochemistry* **2009**, *48*, 4617–4625. [CrossRef] [PubMed]
18. van den Bogaart, G.; Meyenberg, K.; Risselada, H.J.; Amin, H.; Willig, K.I.; Hubrich, B.E.; Dier, M.; Hell, S.W.; Grubmuller, H.; Diederichsen, U.; et al. Membrane protein sequestering by ionic protein-lipid interactions. *Nature* **2011**, *479*, 552–555. [CrossRef]
19. Honigmann, A.; van den Bogaart, G.; Iraheta, E.; Risselada, H.J.; Milovanovic, D.; Mueller, V.; Mullar, S.; Diederichsen, U.; Fasshauer, D.; Grubmuller, H.; et al. Phosphatidylinositol 4,5-bisphosphate clusters act as molecular beacons for vesicle recruitment. *Nat. Struct. Mol. Biol.* **2013**, *20*, 679–686. [CrossRef]
20. Khuong, T.M.; Habets, R.L.; Kuenen, S.; Witkowska, A.; Kasprowicz, J.; Swerts, J.; Jahn, R.; van den Bogaart, G.; Verstreken, P. Synaptic PI(3,4,5)P3 is required for Syntaxin1A clustering and neurotransmitter release. *Neuron* **2013**, *77*, 1097–1108. [CrossRef]
21. Greitzer-Antes, D.; Barak-Broner, N.; Berlin, S.; Oron, Y.; Chikvashvili, D.; Lotan, I. Tracking Ca^{2+}-dependent and Ca^{2+}-independent conformational transitions in syntaxin 1A during exocytosis in neuroendocrine cells. *J. Cell Sci.* **2013**, *126*, 2914–2923. [CrossRef]
22. Vertkin, I.; Styr, B.; Slomowitz, E.; Ofir, N.; Shapira, I.; Berner, D.; Fedorova, T.; Laviv, T.; Barak-Broner, N.; Greitzer-Antes, D.; et al. $GABA_B$ receptor deficiency causes failure of neuronal homeostasis in hippocampal networks. *Proc. Natl. Acad. Sci. USA* **2015**, *112*, E3291–E3299. [CrossRef] [PubMed]
23. Singer-Lahat, D.; Barak-Broner, N.; Sheinin, A.; Greitzer-Antes, D.; Michaelevski, I.; Lotan, I. The dual function of the polybasic juxtamembrane region of syntaxin 1A in clamping spontaneous release and stimulating Ca^{2+}-triggered release in neuroendocrine cells. *J. Neurosci.* **2018**, *38*, 220–231. [CrossRef] [PubMed]
24. Sarno, S.; Reddy, H.; Meggio, F.; Ruzzene, M.; Davies, S.P.; Donella-Deana, A.; Shugar, D.; Pinna, L.A. Selectivity of 4,5,6,7-tetrabromobenzotriazole, an ATP site-directed inhibitor of protein kinase CK2 ('casein kinase-2'). *FEBS Lett.* **2001**, *496*, 44–48. [CrossRef]
25. Kabachinski, G.; Kielar-Grevstad, D.M.; Zhang, X.; James, D.J.; Martin, T.F. Resident CAPS on dense-core vesicles docks and primes vesicles for fusion. *Mol. Biol. cell* **2016**, *27*, 654–668. [CrossRef] [PubMed]

26. Wang, D.; Zhang, Z.; Dong, M.; Sun, S.; Chapman, E.R.; Jackson, M.B. Syntaxin requirement for Ca^{2+}-triggered exocytosis in neurons and endocrine cells demonstrated with an engineered neurotoxin. *Biochemistry* **2011**, *50*, 2711–2713. [CrossRef]

27. Schiavo, G.; Shone, C.C.; Bennett, M.K.; Scheller, R.H.; Montecucco, C. Botulinum neurotoxin type C cleaves a single Lys-Ala bond within the carboxyl-terminal region of syntaxins. *J. Biol. Chem.* **1995**, *270*, 10566–10570. [CrossRef] [PubMed]

28. Bennett, M.K.; Miller, K.G.; Scheller, R.H. Casein kinase II phosphorylates the synaptic vesicle protein p65. *J. Neurosci.* **1993**, *13*, 1701–1707. [CrossRef]

29. Davletov, B.A.; Sudhof, T.C. A single C2 domain from synaptotagmin I is sufficient for high affinity Ca^{2+}/phospholipid binding. *J. Biol. Chem.* **1993**, *268*, 26386–26390. [CrossRef]

30. Nielander, H.B.; Onofri, F.; Valtorta, F.; Schiavo, G.; Montecucco, C.; Greengard, P.; Benfenati, F. Phosphorylation of VAMP/synaptobrevin in synaptic vesicles by endogenous protein kinases. *J. Neurochem.* **1995**, *65*, 1712–1720. [CrossRef]

31. Nojiri, M.; Loyet, K.M.; Klenchin, V.A.; Kabachinski, G.; Martin, T.F. CAPS activity in priming vesicle exocytosis requires CK2 phosphorylation. *J. Biol. Chem.* **2009**, *284*, 18707–18714. [CrossRef] [PubMed]

32. Martin, T.F. PI(4,5)P(2)-binding effector proteins for vesicle exocytosis. *Biochim. Biophys Acta* **2015**, *1851*, 785–793. [CrossRef] [PubMed]

33. Khelashvili, G.; Galli, A.; Weinstein, H. Phosphatidylinositol 4,5-biphosphate (PIP(2)) lipids regulate the phosphorylation of syntaxin N-terminus by modulating both its position and local structure. *Biochemistry* **2012**, *51*, 7685–7698. [CrossRef]

34. Brachet, A.; Leterrier, C.; Irondelle, M.; Fache, M.P.; Racine, V.; Sibarita, J.B.; Choquet, D.; Dargent, B. Ankyrin G restricts ion channel diffusion at the axonal initial segment before the establishment of the diffusion barrier. *J. Cell Biol.* **2010**, *191*, 383–395. [CrossRef] [PubMed]

35. Hien, Y.E.; Montersino, A.; Castets, F.; Leterrier, C.; Filhol, O.; Vacher, H.; Dargent, B. CK2 accumulation at the axon initial segment depends on sodium channel Nav1. *FEBS Lett.* **2014**, *588*, 3403–3408. [CrossRef]

36. Adelman, J.P.; Maylie, J.; Sah, P. Small-conductance Ca^{2+}-activated K^{+} channels: Form and function. *Annu. Rev. Physiol.* **2012**, *74*, 245–269. [CrossRef]

37. Allen, D.; Fakler, B.; Maylie, J.; Adelman, J.P. Organization and regulation of small conductance Ca^{2+}-activated K^{+} channel multiprotein complexes. *J. Neurosci.* **2007**, *27*, 2369–2376. [CrossRef]

38. Kimura, R.; Matsuki, N. Protein kinase CK2 modulates synaptic plasticity by modification of synaptic NMDA receptors in the hippocampus. *J. Physiol.* **2008**, *586*, 3195–3206. [CrossRef] [PubMed]

39. Milovanovic, D.; Platen, M.; Junius, M.; Diederichsen, U.; Schaap, I.A.; Honigmann, A.; Jahn, R.; van den Bogaart, G. Calcium Promotes the Formation of Syntaxin 1 Mesoscale Domains through Phosphatidylinositol 4,5-Bisphosphate. *J. Biol. Chem.* **2016**, *291*, 7868–7876. [CrossRef]

40. Weninger, K.; Bowen, M.E.; Choi, U.B.; Chu, S.; Brunger, A.T. Accessory proteins stabilize the acceptor complex for synaptobrevin, the 1:1 syntaxin/SNAP-25 complex. *Structure* **2008**, *16*, 308–320. [CrossRef]

41. Binda, F.; Dipace, C.; Bowton, E.; Robertson, S.D.; Lute, B.J.; Fog, J.U.; Zhang, M.; Sen, N.; Colbran, R.J.; Gnegy, M.E.; et al. Syntaxin 1A interaction with the dopamine transporter promotes amphetamine-induced dopamine efflux. *Mol. Pharmacol.* **2008**, *74*, 1101–1108. [CrossRef]

42. An, S.J.; Almers, W. Tracking SNARE complex formation in live endocrine cells. *Science* **2004**, *306*, 1042–1046. [CrossRef] [PubMed]

43. Okamoto, K.; Nagai, T.; Miyawaki, A.; Hayashi, Y. Rapid and persistent modulation of actin dynamics regulates postsynaptic reorganization underlying bidirectional plasticity. *Nat. Neurosci.* **2004**, *7*, 1104–1112. [CrossRef] [PubMed]

44. Mosharov, E.V. Analysis of single vesicle exocytosis events recorded by amperometry. *Methods Mol. Biol.* **2008**, *440*, 315–327. [PubMed]

45. Shang, S.; Wang, C.; Liu, B.; Wu, Q.; Zhang, Q.; Liu, W.; Zheng, L.; Xu, H.; Kang, X.; Zhang, X.; et al. Extracellular Ca^{2+} per se inhibits quantal size of catecholamine release in adrenal slice chromaffin cells. *Cell Calcium* **2014**, *56*, 202–207. [CrossRef]